VOL. 20, NO. 2, 2021, 25-32
www.elektrika.utm.my
ISSN 0128-4428

ELEKTRIKA
Journal of Electrical Engineering

Improved Pole-placement Control with Feed-forward Dead Zone Compensation for Position Tracking of Electro-Pneumatic Actuator System

Noorhazirah Sunar[1*], **Mohd Fua'ad Rahmat**[1], **Ahmad 'Athif Mohd Fauzi**[2], **Zool Hilmi Ismail**[3], **Siti Marhanis Osman**[4] and **Siti Fatimah Sulaiman**[5]

[1]Division of Control and Mechatronics Engineering, School of Electrical Engineering, Faculty of Engineering, Universiti Teknologi Malaysia, Johor, Malaysia.
[2]Center for Artificial Intelligence and Robotics, Universiti Teknologi Malaysia, Jalan Sultan Yahya Petra, Malaysia.
[3]Institute/Coe/Rc Malaysia-Japan International Institute of Technology (MJIIT), Department of System Electronic Engineering, UTM Kuala Lumpur, Malaysia.
[4]Faculty of Electrical Engineering Technology Universiti Malaysia Perlis (UniMAP), Perlis Malaysia.
[5]Center for Telecommunication Research and Innovation (CeTRI), Faculty of Electronics and Computer Engineering, Universiti Teknikal Malaysia Melaka.

[*]Corresponding author: noorhazirah.sunar@gmail.com

Abstract: Dead-zone in the valve degraded the performances of the Electro-Pneumatic Actuator (EPA) system. It makes the system difficult to control, become unstable and leads to chattering effect nearest desired position. In order to cater this issue, the EPA system transfer function and the dead-zone model is identified by MATLAB SI toolbox and the Particle Swarm Optimization (PSO) algorithm respectively. Then a parametric control is designed based on pole-placement approach and combine with feed-forward inverse dead-zone compensation. To reduce chattering effect, a smooth parameter is added to the controller output. The advantages of using these techniques are the chattering effect and the dead-zone of the EPA system is reduced. Moreover, the feed-forward system improves the transient performance. The results are compared with the pole-placement control (1) without compensator and (2) with conventional dead-zone compensator. Based on the experimental results, the proposed controller reduced the chattering effect due to the controller output of conventional dead-zone compensation, 90% of the pole-placement controller steady-state error and 30% and 40% of the pole-placement controller with conventional dead-zone compensation settling time and rise time.

Keywords: Dead-Zone, Feed-forward, Parametric Control, Pneumatic Actuator, Position Tracking.

Article History: received 25 May 2021; accepted 12 June 2021; published 28 August 2021.

1. INTRODUCTION

The issue of nonlinearity in the EPA system increased the difficulty to control the position of EPA system. In [1-3], it is found out that the dead-zone is the main factor that causes the loss sensitivity in a control system compared to other nonlinearity in the EPA system such as friction force, air mass flows through the valve and compressibility if air. The presence of the dead-zone need to be compensated so that the rapid response and high precision of the position tracking of the EPA system can be achieved [4-5].

The main drawback of using the theoretical basis of the dynamic EPA system is time consuming. Therefore, the System Identification (SI) approach has become the alternate choices for the researcher to model the EPA system. The SI method is the mathematical model which is developed from the measurement of the system input and system output data. In the SI method, the model structure selection determines the types of the model either it is a linear system or a nonlinear system [6]. Numerous researches developed the EPA model as a linear SI model as applied in [7-9] and a nonlinear SI as in [10-12]. Based on the principle of the SI method, Auto-Regressive Exogenous (ARX) is particularly noted for its ease of estimation and offers mathematical convenience [13].

A Hammerstein system is a particularly suitable to represent the systems as a linear SI model with the known nonlinearity structure. A PSO algorithm was adopted to estimate the dead-zone in the Hammerstein model [14]. The PSO algorithm does not require linearity in the parameter and is suitable to identify the Hammerstein system with the known nonlinearity structure and non-minimum phase system.

Once the EPA model is identified, the next step is the controller design. Numerous studies have been investigated to control the position of the EPA system for instance sliding mode control [15-16], fuzzy and neural network control [12,17], feedback linearization [18-19] and PID control [20-21]. However, Pole-placement (PP) controller is used in this research as it is suitable for

discrete time system can be applied to a polynomial system. Moreover, the PP controller are designed based on the closed-loop characteristics which is affected the stability and the transient response.

Initially, the PP controller has been implemented as an adaptive control to the EPA system with an integrator block to the pole-placement [22-26]. However, the aforementioned approach required fast identification algorithm to converge during each sampling time. Moreover, the dead-zone effect was not accounted in the model which could lead to false model identification that can causes instability of the system.

It has been demonstrated that added an Inverse Dead Zone (IDZ) compensator to the pole-placement controller reduced the steady-state error that caused by valve dead-zone. It acted as a Nonlinear Gain (NG) or also called as NG-IDZ in this study. The method was experimentally validated and compared with the nonlinear proportional derivative (NPID) as presented in [27]. From the study, the steady-state error was improved but it slowed the transient performance.

The Feed-Forward (FF) control is one of the methods that is usually can avoid the slowness of the feedback control [28-29]. In [30-31], Zero Phase Error Tracking control and Zero Magnitude Error Tracking control was adopted to design feedforward control and pole-placement control of the electro-hydraulic shake table. Similar to the adaptive pole-placement controller, this control strategy required fast computation to identify the model. Moreover, the dead-zone effect was not accounted in designing the inverse model of the Feedforward control which could provide the incorrect feedforward control parameter. Instead of using invers transfer function, the feedforward control adopted based on inverse dead zone have been investigated. In [32], the dead-zone model is estimated using fuzzy logic. In [33], feedback error learning is used to identify the fuzzy relational model to design the feedforward control. However, using fuzzy logic approach increased the computation and time-consuming returning even. Instead of using fuzzy logic, a Finite State Machine (FSM) can be used as it can operate and determine which controller parameter is activated at that given point in time [34]. The fast-switching algorithm in FSM is an advantage in designing the Inverse Dead Zone (IDZ) compensator in pneumatic system.

In this paper, the feedforward control based on inverse dead zone model is design using Finite state machine and combine it with the pole-placement controller. The propose method is verified simulation and experimental for several conditions. This study is important to the industrial application because it aims to reduce the dead-zone nonlinearity in valve which is applicable in the most of the industrial automation field.

2. MODELLING OF THE EPA SYSTEM

2.1 System Description

The EPA system test bed used in this research is given in Figure 1. The system contains of (1) an Enfield LS-V15s 5/3 bi-directional proportional control valve, (2) Data acquisition card (NI SCB-68), (3) a double acting pneumatic cylinder (FESTO with 500 mm cylinder stroke), (4) a personal computer and (5) a Jun-Air compressor. The EPA system interfaces with the computer using the MATLAB Real Time window target during the system operation. The computer is used as the command and monitors the position of the piston. The position of the piston is measured using magnetic sensor in the range of 0 V to 10 V. The pressure in the cylinder is controlled by the proportional valve with input of -10 V to 10 V. The supply pressure to the valve is provided by a Jun-Air compressor with 6 kPa pressure.

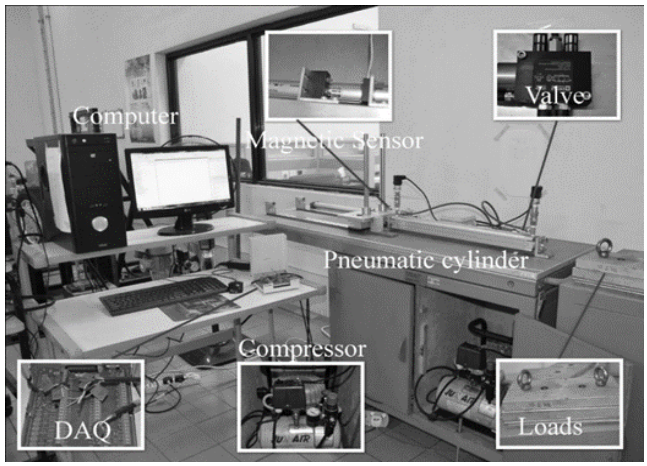

Figure 1. Electro-pneumatic actuator system

2.2 Model Identification

In this study, a Hammerstein model is chosen to identify the mathematical model of the EPA system. It consists of a static nonlinear element and a linear dynamic element which is the dead-zone model and an ARX model. First, the ARX model is identified by using the MATLAB SI toolbox. Then, the dead-zone model parameters are optimized by using the PSO algorithm. More detailed is discussed in the following subsection.

The linear ARX model is obtained by using the SI MATLAB toolbox in the form of:

$$A(z)y(t) = B(z)u(t) + e(t) \tag{1}$$

The dead-zone model in this study is assumed to be asymmetric as depicted in Figure 2. The input to the proportional valve is given by $u(t)$ and the corresponding output $u_d(t)$ is given by the piston movement caused by air flow in the Pressure 1 and Pressure 2. The m_r and m_l are right slope and left slope while b_r, and b_l are right break point and left break point respectively. The input and output relationship of the dead-zone model if given as Equation (2).

$$u_d(t) = \begin{cases} m_l u(t) - m_l b_l & u(t) < b_l \\ 0 & b_l \le u(t) \le b_r \\ m_r u(t) - m_r b_r & u(t) > b_r \end{cases} \tag{2}$$

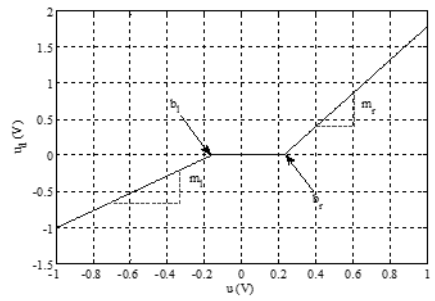

Figure 2. Asymmetric dead-zone model

3. CONTROLLER DESIGN

3.1 Pole-placement Controller

The pole-placement controller used in this study to control the position of the EPA system. The EPA system controlled by pole-placement controller closed loop system is given in Figure 3. From Figure 3, there are two compensation block (1) output compensation and (2) input compensation. The closed loop of the system is given in Equation (3).

$$y(t) = \frac{B(z)H(z)}{A(z)F(z)+B(z)G(z)}r(t) \tag{3}$$

where $A(z)$ and $B(z)$ is the denominator and the numerator of the linear EPA system. Let the characteristic of the desired system is $T(z)$, the Diophantine equation can be defined as Equation (4):

$$A(z)F(z) + B(z)G(z) = T(z) \tag{4}$$

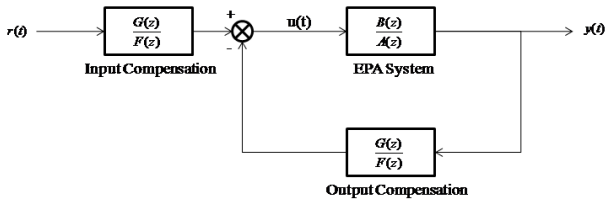

Figure 3. Closed-loop of the EPA system with the pole-placement controller

3.2 Feedforward Inverse Dead Zone

The inverse dead-zone model is used to designed a feedforward compensator. The proposed feedforward control with pole-placement control is represented in Figure 4.

Equation (5) represent the inverse dead-zone as a function of $u_d(t)$. This inverse function will be used to design dead-zone compensator in the proportional valve. This strategy requires only position transducer and open loop experimental data. The PSO algorithm is used to estimate the value of m_r, m_l, b_r and b_l.

$$u(t) = \begin{cases} \dfrac{u_d(t)}{m_l} + b_l & u_d(t) < 0 \\ 0 & u_d(t) = 0 \\ \dfrac{u_d(t)}{m_r} + b_r & u_d(t) > 0 \end{cases} \tag{5}$$

The feedforward control is designed as a switch function which adopted the finite state machine algorithm. Steady-state state is set to 1 ($SE = 1$) when position error is in the steady-state state and controller output is activated. Otherwise, steady-state error is set to 0 ($SE = 0$). From the inverse dead zone model in Equation (5), the left input u_l, and the right input, u_r is triggered when the controller output is less than zero and is greater than zero respectively.

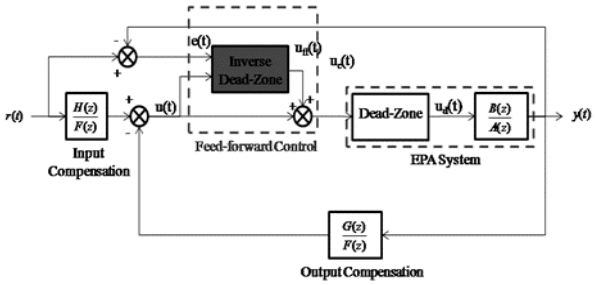

Figure 4. Feed-forward inverse dead-zone with pole-placement controller

The l_c parameter is introduced to smooth the chattering effect. Parameter l_c is set to 1 if the error is far from l_c value. If $l_c = 1$ and $DE = 0$, $u_r = 0$ and $u_l = 1$. If $l_c = 1$ and $DE = 1$, $u_r = 1$ and $u_l = 0$. Regardless of the direction error and states, the u_l and u_r are deactivate when the error is near the l_c parameter. The output of the feed-forward compensator can be formulated as:

$$u_{ff}(t) = lc.\left(\frac{1}{m_r}u(t) + b_r\right)ur.SE.DE + lc.\left(\frac{1}{m_l}u(t) + b_l\right).SE.\overline{DE} \tag{6}$$

3.3 Stability Analysis

Since the model is in z-transform, the Jury Criterion is employed to analyze the stability of the system. First, the model of the dead-zone and inverse dead-zone must transform to the z-domain system. The z-transform of the dead-zone model and its inverse dead-zone model is given in Equation (2) and Equation (3) respectively. The stability analysis is performed when the FFIDZ is activated ($SE = 1$). When $SE = 1$, the controller output $u_c(t)$ in the z-transform is given in Equation (7).

$$U_c(z) = U(z) + \frac{U(z)}{m^*} + \frac{b^*}{1-z^{-1}} \tag{7}$$

where m^* represent the m_r or m_l and b^* represent b_r or b_l. Equation (8) represent the closed-loop of the overall system.

$$\frac{Y(z)}{R(z)} = \frac{(m^*+1)B(z)H(z)}{A(z)F(z)+(m^*+1)B(z)G(z)} \tag{8}$$

4. RESULTS AND DISCUSSIONS

4.1 Estimated EPA model

The third order linear approximation of the ARX model shows the highest best fit percentage which is 95.31%. The third order model is chosen as the EPA model as its best fit percentage is greater than 90% and its loss function and FPE is considered small. The simulation model output and its measured model output is illustrated in Figure 5.

The EPA system was induced with positive and negative input to investigate the valve input and the position output response. The input is limited to the -5V to 5V due to the limitation of the EPA system cylinder stroke. The right break-point, b_r and left break-point, b_l were obtained from the Figure 6 which is 1.232 and -1.722 respectively. The value of m_r and m_l are identified by using the PSO algorithm which is 1.7627 and 1.0707 respectively.

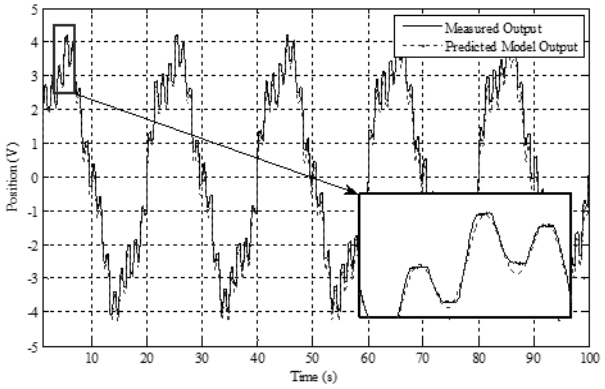

Figure 5. EPA system measured and predicted model output

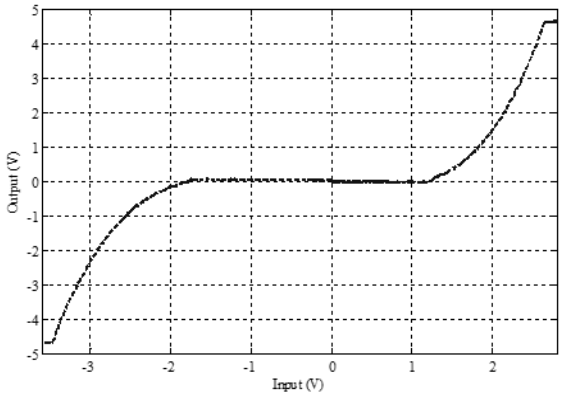

Figure 6. Input response and output response of the EPA system with the dead-zone

The resulted transfer function and dead-zone model of the EPA system are written in Equation (9) and Equation (10) respectively.

$$G_{EPA}\left(z^{-1}\right)=\frac{1.024z^{-1}-2.046z^{-2}+1.029z^{-3}}{1-0.9094z^{-1}-0.6110z^{-2}+0.5204z^{-3}} \quad (9)$$

$$u_d(t)=\begin{cases}1.0701u(t)-1.0707*(-1.722) & u(t)<b_l\\ 0 & b_l\le u(t)\le b_r\\ 1.7627u(t)-1.7627*(1.232) & u(t)>b_r\end{cases} \quad (10)$$

4.2 Numerical Stability Analysis

From the obtained dead-zone model parameter, $b_r = 1.232$, $b_l = -1.722$, $m_r = 1.7627$ and $m_l = 1.0707$. For the controller design specification of two percent overshoot and two seconds settling time, the obtained controller parameter is given by:

$$T(z) = 1 - 2.865z^{-1} + 2.7344z^{-2} - 0.8694z^{-3} \quad (11)$$

$$F(z) = 1 - 1.778z^{-1} + 0.7828z^{-2} \quad (12)$$

$$G(z) = -0.1734 + 0.577z^{-1} - 0.3958z^{-2} \quad (13)$$

As discussed previously in the stability analysis section, the FF-IDZ is activated when u_l or u_r is activated. For condition when u_l is activated, the closed-loop characteristic equation, $P(z)$ is given by:

$$P(z)=z^5-3.0551z^4+3.7470z^3-2.7583z^2+1.5027z-0.4362 \quad (14)$$

Meanwhile, for condition when u_r is activated, the closed-loop characteristic equation is given by:

$$P(z)=z^5-3.1780z^4+4.4014z^3-3.9791z^2+2.4740z-0.7181 \quad (15)$$

Based on Jury stability method, for the mentioned two conditions, all sufficient conditions for stability are satisfied. Thus, the system is stable for the two cases.

4.3 Normal Time Response at Varying Position Distance

The position distance of 25 mm to 200 mm step responses are plotted in Figure 7 to Figure 10. It can be clearly observed from Figure 7 to Figure 10 that the pole-placement controller performance produced a high steady-state error. It is also demonstrated that the time taken for the PP controller to reach 90% of its desired position more than 5 s.

Figure 7 to Figure 10 clearly indicated that rise time and steady-state error was improved by the PP FF-IDZ as the desired position varied from 25 mm to 200 mm. Also, the proposed controller remains with no overshoot as the desired position distance increased. The controller performances of settling, rise time, steady-state error and overshoot percentage are listed in Table 1.

The PP FF-IDZ rise times are 0.24 s, 0.30 s, 0.41 s and 0.34s for 25 mm, 50 mm, 100 mm and 200 mm respectively. Meanwhile, for 25 mm, 50 mm, 100 mm and 200 mm position distance, the resulted rise time are 0.47 s, 0.63 s and 0.68 s respectively. These results demonstrated that the PP FF-IDZ improved in average of 45% of the PP NG-IDZ. Also, the PP FF-IDZ settling time improved up to 56.03% settling time of the EPA system controlled by PP NG-IDZ controller. These results indicated that the PP FF-IDZ improved the performance of the PP NG-IDZ performances in term of settling time and rise time.

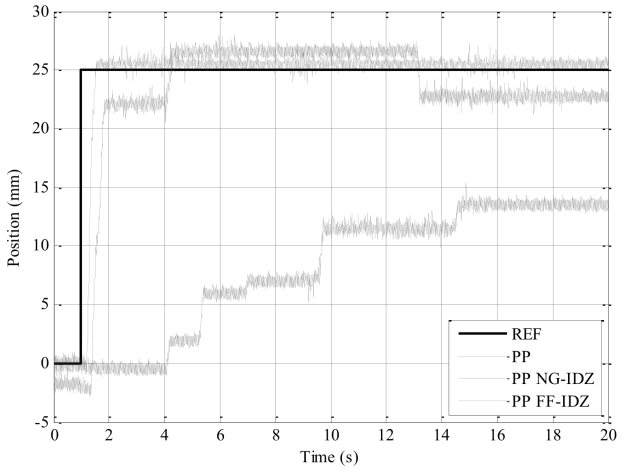

Figure 7. Normal time response for position distance of 25 mm

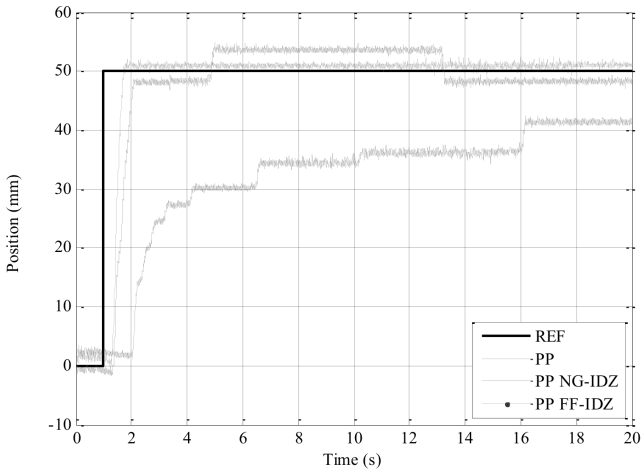

Figure 8. Normal time response for position distance of 50 mm

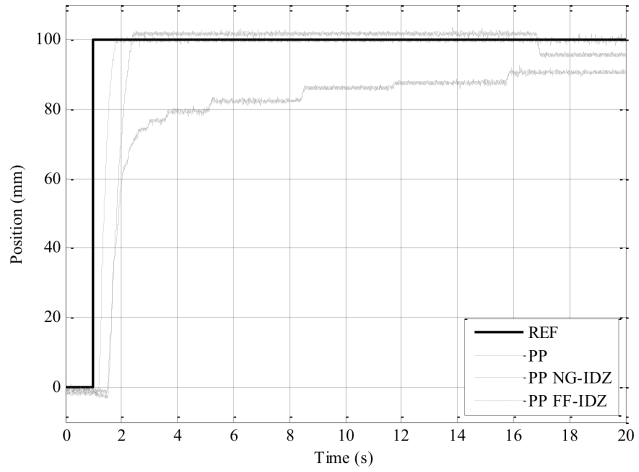

Figure 9. Normal time response for position distance of 100 mm

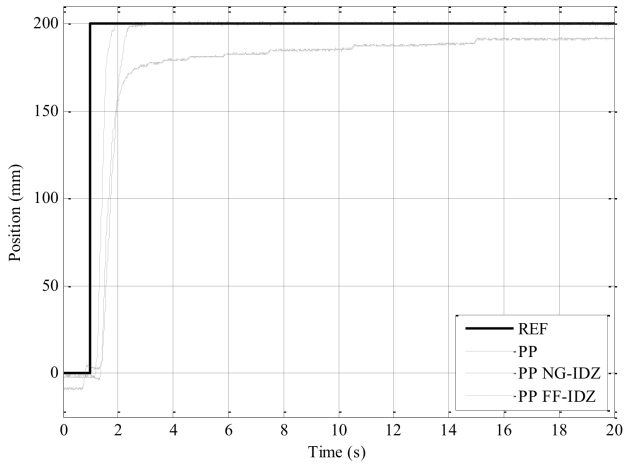

Figure 10. Normal time response for position distance of 200 mm

For the steady-state performance, the PP controller produced an average of 13.79 mm steady-state error for a step input range between 25 mm to 200 mm. However, the PP FF-IDZ reduced 95% of the PP controller steady-state error. This result proved that steady-state error of the PP controller is successfully reduced.

The controller output of PP controller and its position error is given in Figure 11. From Figure 11, at time 1 s to 3 s, the controller output of 25 mm and 50 mm position distance are less than the value of b_r. Therefore, the time duration time for the system to reach 90% of its desired value is longer than 5 s. As the time to $t = 20\,s$, the controller output also less than the value of b_r. Thus, the controller output unable to converge the error near to zero as the time increase to 20 s. The steady-state error of the EPA system controlled by PP controller is in the range of 25 mm.

Table 1. Experimental studies of 25 mm, 50 mm, 100 mm and 200 mm step response controller performance

Reference (mm)	Criterion	PP	PP NG-IDZ	PP FF-IDZ
25	$T_r(s)$	>5	0.47	0.24
	$T_s(s)$	>5	1.16	0.51
	$e_{ss}(mm)$	14.72	1.96	0.67
	$OS(\%)$	0	0	0
50	$T_r(s)$	>5	0.60	0.30
	$T_s(s)$	>5	1.07	0.72
	$e_{ss}(mm)$	13.92	2.84	1.04
	$OS(\%)$	0	0	0
100	$T_r(s)$	14.21	0.63	0.41
	$T_s(s)$	>5	1.35	0.78
	$e_{ss}(mm)$	13.50	2.43	0.46
	$OS(\%)$	0	0	0
200	$T_r(s)$	2.39	0.68	0.34
	$T_s(s)$	>5	1.50	0.81
	$e_{ss}(mm)$	13.02	0.49	0.51
	$OS(\%)$	0	0	0

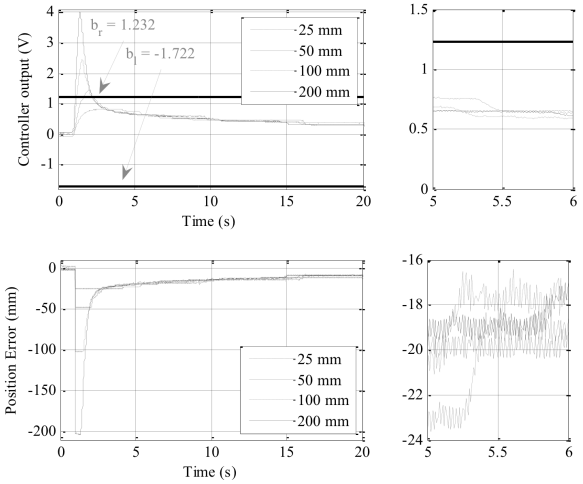

Figure 11. PP controller output response and position error with respect to step input signal.

Figure 12 shows the controller output and the position error of the EPA system controlled by PP NG-IDZ. Figure 12 shows a slight position movement at time 4 s to 13 s for 25 mm, 5 s to 13 s for 50 mm and 16 s to 20 s for 100 mm. The offset handler in the dead-zone compensator caused these inconsistencies. The dead-zone compensator causes the chattering effect to the position output. The steady state error is in between -5 mm to 5 mm.

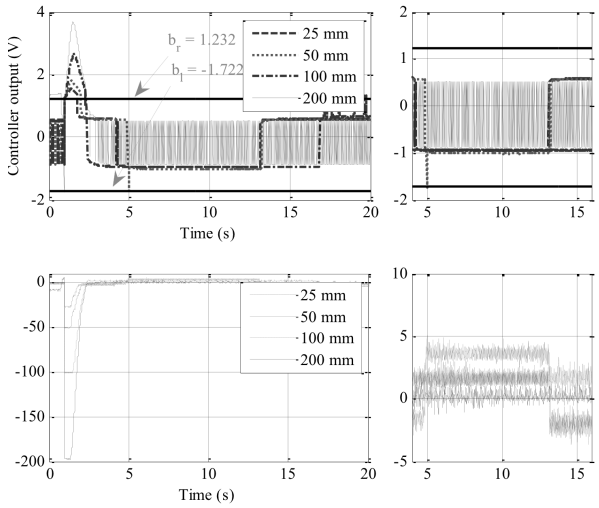

Figure 12. PP NG-IDZ controller output response and position error with respect to step input signal.

Figure 13 illustrated the PP FF-IDZ controller output is greater than b_r time 1 s to 2 s. This leads the rapid time response of the EPA system while preventing the overshoot. Compared the controller output of PP NG-IDZ in Figure 12, controller output of PP FF-IDZ does not have the chattering controller output due to the l_c parameter in the controller. As a result, the position error of the EPA system controlled by PP FF-IDZ does not show the inconsistency. The steady-state error is in between -1 mm to 2 mm. For 200 mm position displacement, the steady-state error of PP FF-IDZ able to improve 3.5% and 16.5% the steady-state error controlled by PP NG-IDZ controller and PP controller respectively.

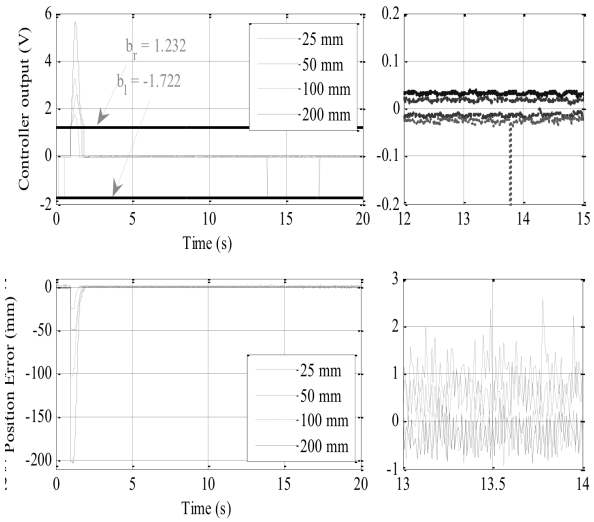

Figure 13. PP FF-IDZ controller output and position error with respect to a step input.

5. CONCLUSION

In this paper, a practical solution to control the position tracking of the EPA system was investigated. The issue highlight in this study is the dead-zone effect in the EPA system and the chattering occurred in the control algorithm in the range near zero error. A new integrated pole-placement controller with inverse dead-zone and a smooth parameter were proposed to overcome this issue. Based on the third order ARX model, the pole-placement was developed. Then, the feedforward dead-zone compensator was designed based on the inverse dead-zone model. Also, a smooth parameter was added to the controller output in order to reduce chattering effect near desired position. The pole-placement controller and pole-placement controller with nonlinear gain inverse dead zone used to compare the performance of the proposed controller in simulation and normal time response at varying position distance. The performance comparison indicated that the proposed control algorithm improved pole-placement controller steady-state error and transient time of the pole-placement controller with nonlinear gain inverse dead-zone controller about 90% and 30% to 40% respectively. These results confirmed that the dead-zone is the main issues in the steady-state performance of the EPA system. These results have successfully indicated that the proposed controller improved the response time and the steady state error performance under varied position distance.

In this study, the proposed control techniques have been significantly improved the performance of the system compared to others conventional techniques. The novelty of this study is the compensation method of the chattering effect due the controller output near zero position error. The added smooth parameter in the control algorithm has been effectively reduced the chattering effect. Furthermore, the designed feed-forward inverse dead-zone

compensator not only reduced the time response, it also reduced the high steady state error. Also, it has been successfully proven that the effectiveness of the proposed method by analyzing the simulation and normal time response performance other control algorithm.

ACKNOWLEDGMENT

This research is supported by the Universiti Teknologi Malaysia (UTM) and Ministry of High Education (MOHE) through GUP grant TIER 1 vote number Q.JI30000.2523.00H36 which is greatly appreciated. The authors are grateful for the MyPhD scholarship under the MyBrain 15 program by MOHE for author scholarship.

REFERENCES

[1] J. H. Pérez-Cruz, I. Chairez, J. d. Jesús Rubio and J. Pacheco, "Identification and control of class of non-linear systems with non-symmetric deadzone using recurrent neural networks," *IET Control Theory & Applications*, vol. 8, pp. 183-192, 2014.

[2] A. Sobczyk, "Construction machines and manipulators: modern designs and research problems," *Developments in fluid power control of machinery and manipulators, Cracow: Fluid Power Net Publication*, pp. 345-364, 2000.

[3] A. C. Valdiero, R. Guenther, and V. J. De Negri, "New methodology for identification of the dead zone in proportional directional hydraulic valves," *Proc. Proceedings of the 18th Brazilian Congress of Mechanical Engineering*, São Paulo, Brazil: COBEM, 2005, pp. 377-384.

[4] Z. J. Zhang, "A Robust Controller for Positioning Control of Pneumatic Servo System: Design and Experiment Tests," *Applied Mechanics and Materials, Trans Tech Publications, Ltd.*, vol. 668–669, pp. 423–427, 2014.

[5] D. Kaiser, S. Engineer, and P. Compumotor, "Fundamentals of Servo Motion Control," 2001.

[6] I. M. Yassin, M. N. Taib and R. Adnan, "Recent Advancements and Methodologies in System Identification: A Review," *Scientific Research Journal*, vol. 1, pp. 14-33, 2013

[7] M.-C. Shih and S.-I. Tseng, "Identification and position control of a servo pneumatic cylinder," *Control Engineering Practice*, vol. 3, pp. 1285-1290, 1995.

[8] Y. Wang, T. Deng, Li, J. and G. Bao, "Research on variable gain feedforward trajectory control of pneumatic servo system," *Proc. 2015 International Conference on Fluid Power and Mechatronics (FPM), IEEE*, 2015, pp. 350-354.

[9] A. Saleem, B. Taha, T. Tutunji and A. Al-Qaisia, "Identification and cascade control of servo-pneumatic system using Particle Swarm Optimization," *Simulation Modelling Practice and Theory*, vol. 52, pp. 164-179, 2015.

[10] T. Vesselenyi, S. Dzitac, I. Dzitac and M. J. Manolescu, "Fuzzy and neural controllers for a pneumatic actuator," *International Journal of Computers, Communications and Control*, vol. 2, pp. 375-387, 2007.

[11] S. Kaitwanidvilai and P. Olranthichachat, "Robust loop shaping-fuzzy gain scheduling control of a servo-pneumatic system using particle swarm optimization approach," *Mechatronics*, 2010.

[12] H. Schulte, and H. Hahn, "Fuzzy state feedback gain scheduling control of servo-pneumatic actuators," *Control Engineering Practice*, vol. 12, pp. 639-650, 2004.

[13] A. K. Tangirala, *Principles of system identification: theory and practice*, Crc Press, 2014.

[14] H. N. Al-Duwaish, "Identification of Hammerstein Models with Known Nonlinearity Structure Using Particle Swarm Optimization," *Arab J Sci Eng*, vol. 36, pp. 1269-1276, 2011.

[15] E. Richer and Y. Hurmuzlu, "A High Performance Pneumatic Force Actuator System: Part II---Nonlinear Controller Design," *Journal of dynamic systems, measurement, and control*, vol. 122, no. 3, pp. 426-434, 2000.

[16] J. F. Carneiro, and F. G. de Almeida, "Accurate motion control of a servopneumatic system using integral sliding mode control," *The International Journal of Advanced Manufacturing Technology*, pp. 1-16, 2014.

[17] Q. Song, F. Liu and R. D. Findlay, "Improved Fuzzy Neural Network Control for a Pneumatic System Based on Extended Kalman Filter," *Proc. International Conference on Computational Intelligence for Modelling Control and Automation and International Conference on Intelligent Agents Web Technologies and International Commerce (CIMCA'06)*, Sydney, NSW, Australia, 2006, pp. 76-76.

[18] F. Xiang and J. Wikander, "Block-oriented approximate feedback linearization for control of pneumatic actuator system," *Control Engineering Practice*, vol. 12, no. 4, pp. 387-399, 2004.

[19] T. Kimura, S. Hara, T. Fujita and T. Kagawa, "Feedback linearization for pneumatic actuator systems with static friction," Control Engineering Practice, vol. 5, no. 10, pp. 1385-1394, 1997.

[20] Z. Situm, D. Pavkovic and B. Novakovic, "Servo Pneumatic Position Control Using Fuzzy PID Gain Scheduling," *Journal of dynamic systems, measurement, and control*, vol. 126, no. 2, pp. 376-387, 2004.

[21] P. Zítek, J. Fišer and T. Vyhlídal, "Dimensional analysis approach to dominant three-pole placement in delayed PID control loops," *Journal of Process Control*, vol. 23, no. 8, pp. 1063-1074, 2013.

[22] J. Bobrow, and F. Jabbari, "Adaptive pneumatic force actuation and position control," *ASME J. Dyn. Syst., Meas., Control*, vol. 113, no.2, pp. 267-272, 1991.

[23] M.-C. Shih, and Y.-F. Huang, "Pneumatic Servo-Cylinder Position Control Using a Self-Tuning Controller," *JSME international journal. Ser. 2, Fluids engineering, heat transfer, power, combustion, thermophysical properties*, vol. 35, no. 2, pp. 247-254, 1992.

[24] D. G. Caldwell, G. A. Medrano-Cerda and M. Goodwin, "Characteristics and adaptive control of pneumatic muscle actuators for a robotic elbow," *Proc. Proceedings of the 1994 IEEE International*

Conference on Robotics and Automation, San Diego, CA, USA, 1994, vol.3554, pp. 3558-3563.

[25] K. Tanaka, Y. Yamada, A. Shimizu and S. Shibata, "Multi-rate adaptive pole-placement control for pneumatic servo system with additive external forces," *Proc. Advanced Motion Control*, AMC '96-MIE. Proceedings., 1996 4th International Workshop on, Mie, Japan, 1996, vol. 211, pp. 213-218.

[26] Y. Yamada, K. Tanaka and S. Uchikado, "Adaptive pole-placement control with multi-rate type neural network for pneumatic servo system," *Proc. Proceedings of the 2000. IEEE International Conference on Control Applications. Conference Proceedings (Cat. No.00CH37162),* Anchorage, AK, USA, 2000, pp. 190-195.

[27] N. H. Sunar, M. F. Rahmat, S. N. S. Salim, Z. H. Ismail and A. A. M. Fauzi, "Model Identification and Controller Design for an Electro-Pneumatic Actuator System with Dead Zone Compensation," *International Journal On Smart Sensing and Intelligent Systems*, vol. 7, no. 2, pp. 21, 2014.

[28] H. Hussein, "Feedforward, Hot and Cold Control System for Controlling Plastic Insulation Thickness in Manufacturing of Cable Products," *Arab J Sci Eng*, vol. 39, no. 2, pp. 1399-1408, 2014.

[29] S. Mohamed, A. Zayed and O. Abolaeha, "New Feed-Forward/Feedback Generalized Minimum Variance Self-tuning Pole-placement Controller," *Proceedings of World Academy of Science: Engineering & Technology*, 2009, vol. 49.

[30] S. Gang, Z. Zhen-Cai, Z. Lei, T. Yu, Y. Chi-fu, Z. Jin-song, L. Guang-da and H. Jun-Wei, "Adaptive feed-forward compensation for hybrid control with acceleration time waveform replication on electro-hydraulic shaking table," *Control Engineering Practice*, vol. 21, no. 8, pp. 1128-1142, 2013.

[31] Y. Tang, Z.-C. Zhu, G. Shen and X. Li, "Improved feedforward inverse control with adaptive refinement for acceleration tracking of electro-hydraulic shake table," *Journal of Vibration and Control*, vol. 22, no. 19, pp. 3945-3964, 2016.

[32] C.-C. Chiang, "Adaptive Fuzzy Tracking Control for Uncertain Nonlinear Time-Delay Systems with Unknown Dead-Zone Input," *Mathematical Problems in Engineering*, 2013, p. 13.

[33] M. Kadri, "Disturbance Rejection in Nonlinear Uncertain Systems Using Feedforward Control," *Arab J Sci Eng*, vol. 38, no. 9, pp. 2439-2450, 2013.

[34] J. E. Seem, G. M. Decious, C. Lomonaco, and A. Bernaden, "Hybrid finite state machine environmental system controller," Google Patents, 2002.